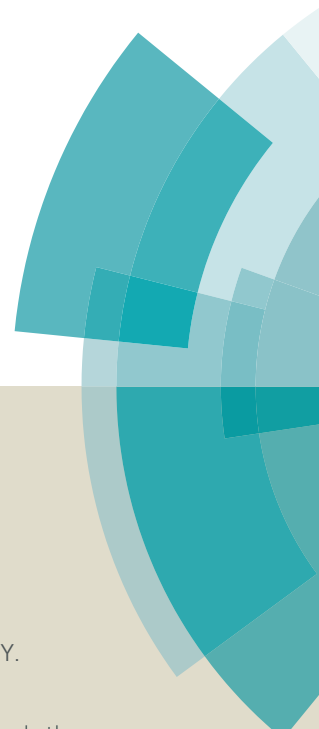
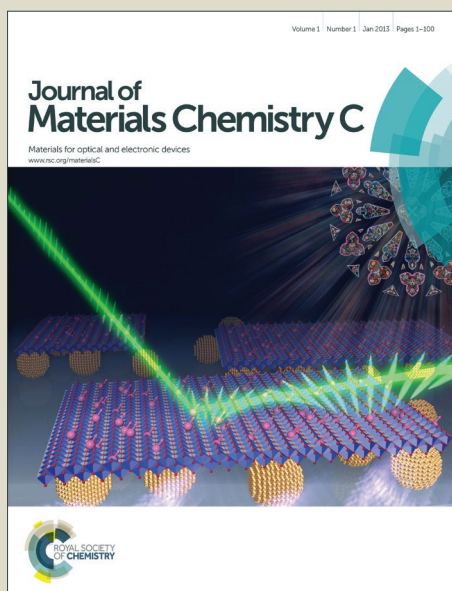


Journal of Materials Chemistry C

Accepted Manuscript



This article can be cited before page numbers have been issued, to do this please use: X. Liu, F. Liang, Y. Yuan, Z. Jiang and L. Liao, *J. Mater. Chem. C*, 2016, DOI: 10.1039/C6TC02180H.



This is an *Accepted Manuscript*, which has been through the Royal Society of Chemistry peer review process and has been accepted for publication.

Accepted Manuscripts are published online shortly after acceptance, before technical editing, formatting and proof reading. Using this free service, authors can make their results available to the community, in citable form, before we publish the edited article. We will replace this *Accepted Manuscript* with the edited and formatted *Advance Article* as soon as it is available.

You can find more information about *Accepted Manuscripts* in the [Information for Authors](#).

Please note that technical editing may introduce minor changes to the text and/or graphics, which may alter content. The journal's standard [Terms & Conditions](#) and the [Ethical guidelines](#) still apply. In no event shall the Royal Society of Chemistry be held responsible for any errors or omissions in this *Accepted Manuscript* or any consequences arising from the use of any information it contains.

ARTICLE

Utilizing 9,10-Dihydroacridine and Pyrazine-Containing Donor-Acceptor Host Materials for High Efficient Red Phosphorescent Organic Light-Emitting Diodes

Cite this: DOI: 10.1039/x0xx00000x

Received 00th January 2012,
Accepted 00th January 2012

DOI: 10.1039/x0xx00000x

www.rsc.org/

Xiang-Yang Liu, Feng Liang, Yi Yuan, Zuo-Quan Jiang,* Liang-Sheng Liao*

Two novel materials 10-(6-(dibenzo[b,d]furan-1-yl)pyrazin-2-yl)-9,9-diphenyl-9,10-dihydroacridine (PrFPhAc) and 10-(6-(dibenzo[b,d]thiophen-1-yl)pyrazin-2-yl)-9,9-diphenyl-9,10-dihydroacridine (PrTPhAc) were designed and synthesized by introducing heterocyclic pyrazine between 9,10-dihydroacridine and dibenzofuran/dibenzothiophene moieties. The basic properties, such as thermal, photophysical and electrochemical properties, were systematically investigated and compared. Both materials have suitable triplet energies for red phosphorescent organic light-emitting diodes, and dibenzofuran (DBF) derivative PrFPhAc was finally achieved superior external quantum efficiency of 22%.

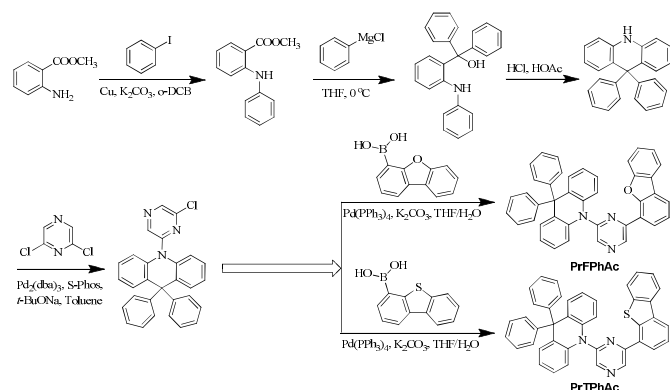
Introduction

Organic light-emitting diodes (OLEDs), since invented in 1987,¹ have attracted massive attention due to their superior potential applications in lighting and display.² In the early stage of OLEDs, it is commonly known that the process of charge recombination to form singlet and triplet excitons was controlled by spin statistics and the ratio of singlet to triplet excitons formed is 1:3, thus the internal quantum efficiency (IQE) of OLEDs was limited within 25% in theory and nearly 75% triplet excitons was wasted.³ It is clear that if one pathway can improve the utilization ratio of triplet excitons, the quantum efficiency of OLEDs will be quadrupled ideally. Fortunately, by using heavy metal complex (such as, iridium or platinum) as emitters doped into the organic matrix can break the law of spin statistics via strong spin-orbit coupling effect, OLEDs can achieve nearly 100% IQE by harvesting both singlet and triplet excitons through fast intersystem crossing (ISC) process.^{3,4} Because this mechanism normally requires the phosphorescent emitters to be doped into an appropriate host to avoid several triplet excitons quenching processes, such as aggregation-caused quenching (ACQ) and triplet-triplet annihilation (TTA). Thus, host matrix is indispensable in highly efficient phosphorescent OLEDs (PHOLEDs). For a good host material for PHOLEDs, favorable electroactivity and suitable excited energy are required for confining triplet excitons in dopants and suppressing triplet-involved quenching effects has been one of the significant challenges.^{5,6}

Generally speaking, red phosphors will suffer from much worse triplet-involved quenching processes as compared to blue and green phosphors due to their high polarity, narrow energy gap (E_g), and longer exciton lifetime, which result in serious device efficiency reduction.⁶ And even with a light-doping device configuration, which will also lead to remarkable triplet quenching effects between host-host and host-guest molecules.^{4d,6,7} Although red PHOLEDs have been studied widely, there are still some important issues to be resolved, such as triplet quenching and carrier trapping processes and one challenge of them is designing suitable host.^{6c} Up to now, only a few of red phosphorescent host materials have been reported with good electroluminescent (EL) performance.^{6c,8} But the triplet states are normally distributed on the charge transport groups, which will simultaneously be involved in triplet quenching process and further speed up the efficiency roll-off.^{6c} For a suitable host material for red PHOLEDs, good thermal stability, high triplet energy (E_T , at least higher than that of red phosphors) and suitable energy level are necessary. Besides, balanced charge transporting ability is also demanded.⁹ In this contribution, we designed and synthesized two novel red host materials 10-(6-(dibenzo[b,d]furan-1-yl)pyrazin-2-yl)-9,9-diphenyl-9,10-dihydroacridine (PrFPhAc) and 10-(6-(dibenzo[b,d]thiophen-1-yl)pyrazin-2-yl)-9,9-diphenyl-9,10-dihydroacridine (PrTPhAc). We selected 9,10-dihydro-acridine as the donor group to facilitate hole injection and two appended phenyl rings to enhance molecular thermal stability. On the other hand, electron-deficient pyrazine along with dibenzofuran (DBF) or dibenzothiophene (DBT) are introduced in *ortho*-

ARTICLE

linking direction. Experimental results showed that both materials presented good thermal stability and suitable triplet energy for red phosphorescent emitters, which qualified them as host materials for red PHOLEDs. Therefore, bis(2-methyl-dibenzo-[f,h]-quinoxaline) Ir(III) (acetylacetonate) (Ir(MDQ)₂(acac)) doped devices were fabricated. As a result, the champion external quantum efficiency (EQE) of 22% was achieved by PrFPhAc based device.



Scheme 1 Molecular structure and synthetic routes of PrFPhAc, and PrTPhAc.

Results and discussions

Synthesis and characterization

Syntheses of 10-(6-(dibenzo[b,d]furan-1-yl)pyrazin-2-yl)-9,9-diphenyl-9,10-dihydroacridine (PrFPhAc) and 10-(6-(dibenzo[b,d]thiophen-1-yl)pyrazin-2-yl)-9,9-diphenyl-9,10-dihydroacridine (PrTPhAc) are outlined in Scheme 1. The key intermediate of 9,9-diphenyl-9,10-dihydroacridine was synthesized according to our previous work.²¹ Then it was readily converted to 10-(6-chloropyrazin-2-yl)-9,9-diphenyl-9,10-dihydroacridine through the classic Buchwald–Hartwig C–N coupling reaction between. At last, the final products (PrFPhAc and PrTPhAc) can be obtained via Pd-catalyzed Suzuki–Miyaura coupling reaction between 10-(6-chloropyrazin-2-yl)-9,9-diphenyl-9,10-dihydroacridine and the corresponding boronic acid of dibenzofuran (DBF) and dibenzothiophene (DBT) in good yields.

Photophysical property

The UV-vis absorption and photoluminescence (PL) spectra of these materials were measured at room temperature in toluene solution and the phosphorescence (Phos) spectra were measured in 2-methyltetrahydrofuran (2-MeTHF) matrix at low temperature (77 K). The detailed data are shown in Fig. 1 and summarized in Table 1. Their UV-vis absorption spectra are quite similar with the maximum peaks and shoulders for PrFPhAc and PrTPhAc, respectively. The absorption peaks at 301 and 296 nm could be attributed to the $n \rightarrow \pi^*$ transitions of the 9,10-dihydroacridine chromophore. The shoulder peaks at around 370 nm (369 and 379 nm) can be attributed to $\pi \rightarrow \pi^*$ transitions of the pyrazine. Besides, the absorption onset of

PrFPhAc is red-shifted by 6 nm as compared to that of PrTPhAc (from 412 to 418 nm).

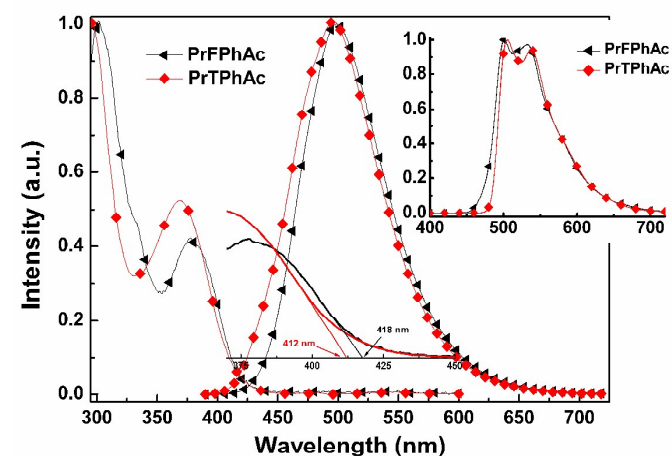


Fig. 1 Room-temperature UV-vis absorption and PL spectra in toluene solution, and Phos spectra in 2-MeTHF matrix at 77 K (inset).

The PL spectra of PrFPhAc and PrTPhAc are peak at 498 and 496 nm, respectively. Furthermore, the PL emission is nearly symmetric, featureless and spectrally broader, which is likely to be correlated to the charge-transfer nature of these materials.¹⁰ Fig. 1 (inset) also shows the Phos spectra of both materials in 2-MeTHF matrix. PrFPhAc and PrTPhAc exhibited the highest vibronic bands at around 502 and 504 nm, corresponding to E_T of 2.47 and 2.46 eV, respectively. These results indicated both materials could be developed for hosting red emitter in PHOLEDs.

Thermal property

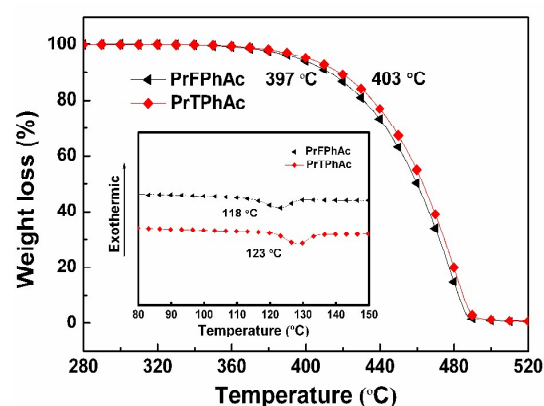


Fig. 2 TGA and DSC (inset) curves of PrFPhAc and PrTPhAc.

A donor-acceptor configuration cannot only bring the ICT effect but also increase the intermolecular force, reflected by the thermal property. As shown in Fig. 2, we found both PrFPhAc and PrTPhAc showed high glass transition temperature (T_g), 118 °C for the former and 123 °C for the

latter. The appending phenyl rings to construct 3-D configuration can be partly responsible for this result, but the T_g s are still over 20 °C higher than those of the host materials with the similar structure with the benzene instead of pyrazine as the central core.²ⁱ Thus, the stronger intermolecular interaction following the increased molecular polarity also contributed to better morphological stability.^{8f,11} It was worth

noting that both molecules showed similar thermal decomposition temperatures (T_d , corresponding to 5% weight loss, Fig. 2) with 397 and 403 °C for PrFPhAc and PrTPhAc, with tiny differences between the phenyl-core materials,²ⁱ which indicated that the molecular size was the major determinant for thermal stability.

Table 1 Summary of the physical properties of PrFPhAc and PrTPhAc.

Host	Abs ^a	PL ^a	T_g^b	T_d^c	E_g^d	E_T^e	HOMO/LUMO ^f
	[nm]	[nm]	[°C]	[°C]	[eV]	[eV]	[eV]
PrFPhAc	301, 377	498	118	397	2.97	2.47	-6.04/-3.07
PrTPhAc	296, 373	496	123	403	3.00	2.46	-6.02/-3.02

a) Measured in toluene solution at room temperature. b) T_g : Glass transition temperature. c) T_d : Decomposition temperature. d) E_g : Band gaps, calculated from the corresponding absorption onset. e) E_T : Measured in 2-MeTHF glass matrix at 77 K. f) HOMO levels, calculated from UPS data. g) LUMO levels calculated from the HOMOs and corresponding E_g s.

Theoretical calculations

DFT calculations were utilized to simulate the frontier molecular orbital (FMO) spatial distributions at a B3LYP/6-31G(d) level for the structure of PrFPhAc and PrTPhAc. As Fig. 3 shows, both molecule have similar HOMO distributions, which are almost localized at the electron-rich 9,10-dihydroacridine centers, while the LUMOs of PrFPhAc and PrTPhAc are distributed on the pyrazine core and the phenyl in each DBF and DBT. As to the specific values of HOMO and LUMO levels, we can found that both materials had very close HOMO because of the same dihydroacridine donor dominated the HOMO distributions, and only 0.03 eV difference was observed. On the other hand, the 0.15 eV difference in LUMO can be attributed to the different acceptor groups, whereas the O atom in DBF had stronger electronegativity than S atom in DBT and thus lead to relatively lower LUMO of PrFPhAc. In general, the PrFPhAc possessed slightly narrower bandgap as compared to PrTPhAc, which was consistent with the UV spectra. Besides, the singlet and triplet energy difference (ΔE_{ST}) were also calculated to be 0.34 and 0.41 eV for PrFPhAc and PrTPhAc, respectively.

Electrochemical properties and HOMO/LUMO levels

The electrochemical properties of PrFPhAc and PrTPhAc were firstly measured by cyclic voltammetry (CV) using typically tri-electrode configuration method with ferrocene as the internal standard in dichloromethane solution with 0.1 M *n*-Bu₄NPF₆ as the supporting electrolyte (Fig. 4). We calculated the HOMO levels of PrFPhAc and PrTPhAc as -5.50 and -5.48 eV, respectively, from the onset of the first oxidation wave.

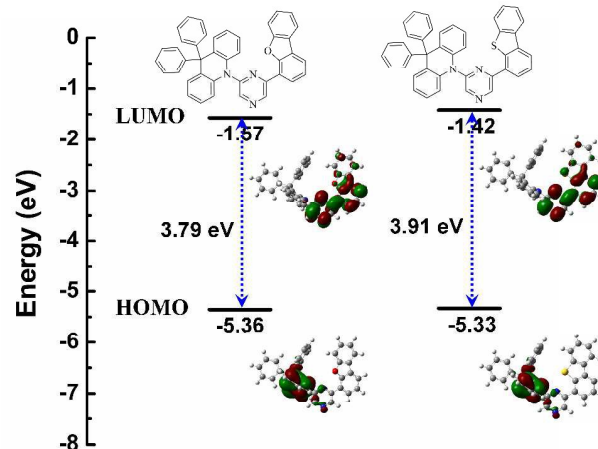


Fig. 3 HOMO/LUMO spatial distributions and optimized geometry.

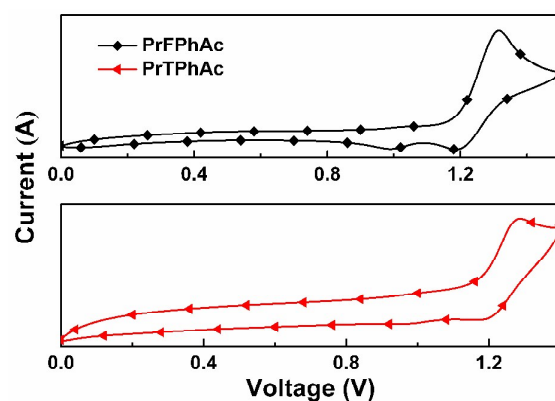


Fig. 4 Cyclic voltammograms of PrFPhAc and PrTPhAc.

The more reliable HOMOs of these materials were tested by ultraviolet photoemission spectroscopy (UPS, Fig. 5) next. The

HOMOs can be determined as follows: $E_{\text{HOMO}} = E_k - hv$, where, hv is the light energy of the light source (normally $hv = 21.22$ eV); E_k is the kinetic energy distribution of the photo-electrons. The LUMOs can be calculated by $E_{\text{LUMO}} = E_g + E_{\text{HOMO}}$, E_g is the optical energy gap and measured by UV-vis absorption spectra. As a result, the HOMO/LUMO levels were measured as -6.04/-3.07 and -6.02/-3.02 eV for PrFPhAc and PrTPhAc, respectively. Overall, the UPS studies is consistent with DFT calculation and CV results in trend.

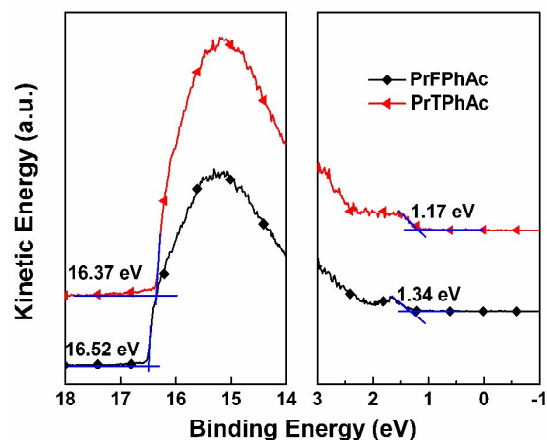


Fig. 5 UPS spectra of PrFPhAc and PrTPhAc.

To investigate the electroluminescence characteristics of these materials, red PHOLEDs were fabricated with typical device structure as following: ITO/HAT-CN (10 nm)/TAPC (45 nm)/TCTA (10 nm)/Host: 4 wt% Ir(MDQ)₂(acac) (20 nm)/TmPyPB (45 nm)/Liq (2 nm)/Al (120 nm). PrFPhAc and PrTPhAc were doped with 4% Ir(MDQ)₂(acac) to form the emitting layer (EML). The current density–voltage–luminance (J – V – L) characteristics; current efficiency (CE), power efficiency (PE) and external quantum efficiency (EQE) as a function of luminance and electroluminescence (EL) spectra of red devices are included in Fig. 6. The detailed performance is summarized in Table 2.

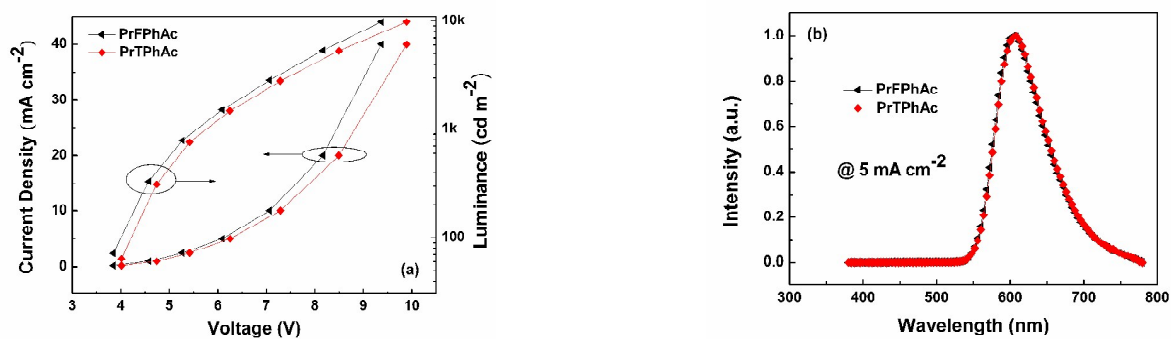
As Fig. 6 (a) shows, the operating voltage PrFPhAc-based OLED at 100 cd m^{-2} is 3.9 V, which is lower than the device hosted by PrTPhAc (4.1 V). As shown in Fig. 5 (b), both devices exhibited the identical emission with conventional CIE coordinates of (0.61, 0.39) of Ir(MDQ)₂(acac). And in Fig. 6 (c), the maximum CE, PE and EQE reached 32.0 cd A^{-1} , 23.1 lm W^{-1} , and 19.2%, respectively, for PrTPhAc-based device. The device based on PrFPhAc showed better performance with 36.0 cd A^{-1} , 29.1 lm W^{-1} and 22.0% for CE, PE and EQE, respectively. Additionally, we carried hole-only and electron-only measurements for two hosts, and PrFPhAc exhibited better hole and electron transport ability as compared to PrTPhAc (Fig. 7), which could be an important reason why the PrFPhAc is superior to PrTPhAc in OLED devices.

Electroluminescence properties

Table 2 Summary of electroluminescence performance for red PHOLEDs.

Host ^a	V ^b	η_{CE}^c	η_{PE}^c	η_{ext}^c	CIE ^d
	[V]	[cd A^{-1}]	[lm W^{-1}]	[%]	[x, y]
PrFPhAc	3.9	36.0, 30.9, 27.2	29.1, 17.7, 10.0	22.0, 19.1, 16.4	0.61, 0.39
PrTPhAc	4.1	32.0, 29.8, 26.7	23.1, 16.7, 9.9	19.2, 18.2, 16.1	0.61, 0.39

a) Device configuration: ITO/HAT-CN (10 nm)/TAPC (45 nm)/TCTA (10 nm)/HOST: 4 wt % Ir(MDQ)₂(acac) (20 nm)/TmPyPB (45 nm)/Liq (2 nm)/Al (120 nm). b) Voltages at 100 cd m^{-2} . c) Efficiencies in the order of the maxima, at 1000 cd m^{-2} and at 5000 cd m^{-2} . d) Commission International de l'Éclairage coordinates measured at 5 mA cm^{-2} .



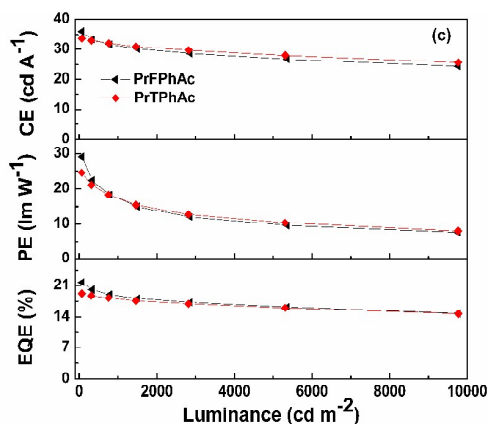


Fig. 6 (a) J - V - L characteristics; (b) EL spectra and (c) CE-, PE- and EQE- L curves of red PHOLEDs.

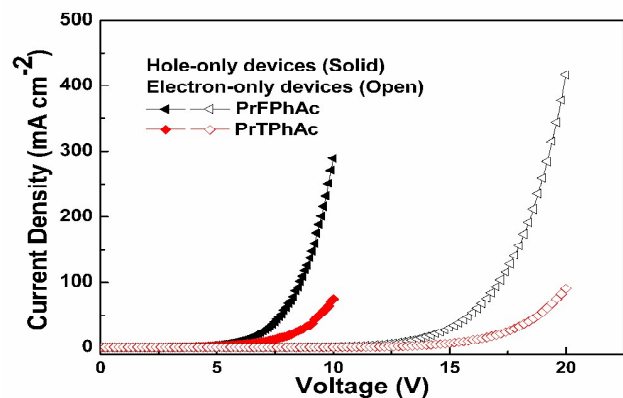


Fig. 7 J - V characteristics of hole-only and electron-only devices. Hole-only device: ITO/MoO₃ (10 nm)/Host (100 nm)/MoO₃ (10 nm)/Al (100 nm); electron-only device: ITO/TmPyPB (20 nm)/Host (100 nm)/ TmPyPB (20 nm)/Liq (2 nm)/Al(100 nm).

Experimental Section

Materials and methods

All chemicals and reagents were used as received from commercial sources without further purification. THF was purified by PURE SOLV (Innovative Technology) purification system. ¹H NMR and ¹³C NMR spectra were recorded on a Bruker 400 spectrometer at room temperature. Mass spectra were recorded on a Thermo ISQ mass spectrometer using a direct exposure probe. UV-vis absorption spectra were recorded on a Perkin Elmer Lambda 750 spectrophotometer. PL spectra and phosphorescent spectra were recorded on a Hitachi F-4600 fluorescence spectrophotometer. Differential scanning calorimetry (DSC) was performed on a TA DSC 2010 unit at a heating rate of 10 °C min⁻¹ under nitrogen. The glass transition temperatures (T_g) were determined from the second heating scan. Thermogravimetric analysis (TGA) was performed on a TA SDT 2960 instrument at a heating rate of 10 °C min⁻¹ under nitrogen. Temperature at 5% weight loss was used as the decomposition temperature (T_d). The DFT simulations were carried out with different parameters for structure optimizations

and vibration analyses. The ground states and triplet states of molecules in vacuum were optimized without any assistance of experimental data by the restricted and unrestricted formalism of three-parameter hybrid exchange functional and correlation functional (B3LYP)/6-31G(d), respectively.¹² All computations were performed using the Gaussian 03 package. Transient PL decays were measured by a single photon counting spectrometer from HORIBA JOBIN YVON with a Nano LED pulse lamp as the excitation source. Cyclic voltammetry (CV) was carried out on a CHI600 voltammetric analyzer at room temperature with ferrocenium-ferrocene (Fc⁺/Fc) as the internal standard.

Device fabrication and measurements

The OLEDs were fabricated through vacuum deposition of the materials at *ca.* 2×10⁻⁶ Torr onto commercially available ITO-coated glass substrates having a sheet resistance of *ca.* 30 Ω per square. The ITO surface was cleaned sequentially with acetone, ethanol, and deionized water, in an ultrasonically bath, dried in an oven, and finally exposed to UV-ozone for about 15 min. Organic layers were deposited at a rate of 2-3 Å/s, subsequently, HAT-CN and Liq were deposited at 0.2-0.3 Å/s, finally the Al electrode was deposited (*ca.* 5 Å/s) through a shadow mask without breaking the vacuum. For all the devices, the emitting areas were determined by the overlap of two electrodes as 0.09 cm². The EL performance of the blue and white devices were measured with a PHOTO RESEARCH SpectraScan PR 655 PHOTOMETER and a KEITHLEY 2400 SourceMeter constant current source at room-temperature. The EQE values were calculated according to the previously reported methods.

Synthesis of 10-(6-chloropyrazin-2-yl)-9,9-diphenyl-9,10-dihydroacridine

9,9-diphenylacridane²¹ (10 g, 30 mmol), 2,6-dichloropyrazine (4.47 g, 30 mmol), tris(dibenzylideneacetone)dipalladium(0) (Pd₂(dba)₃, 0.27 g, 0.3 mmol), 2-dicyclohexylphosphino-2',6'-dimethoxy-1,1'-biphenyl (S-Phos, 0.37 g, 0.9 mmol), sodium *t*-butoxide (*t*-BuONa, 5.76 g, 60 mmol) were dissolved in toluene under argon and heated to 110 °C. After 20 h reaction under stirring, the reaction was cooled to room temperature and 200 mL water was added. The product was extracted with dichloromethane (DCM, 3×100 mL), the combined organic layers were washed with brine and dried over anhydrous sodium sulfate (NaSO₄). Filtered and evaporated under reduced pressure. The crude product was purified by column chromatography using petroleum ether/dichloromethane (2/1, v/v) to give 10-(6-chloropyrazin-2-yl)-9,9-diphenyl-9,10-dihydroacridine as a white crystalline powder (4.3 g, 32%). ¹H NMR (400 MHz, CDCl₃): δ 7.89 (s, 1H), 7.76 (dd, J = 8.0, 1.0 Hz, 2H), 7.61 (s, 1H), 7.38 (m, 2H), 7.22-7.17 (m, 10H), 7.01 (m, 2H), 6.88 (d, J = 3.8 Hz, 2H) ppm. ¹³C NMR (100 MHz, CDCl₃): δ 151.48, 145.52, 144.02, 141.80, 140.01, 134.69, 131.64, 130.38, 129.10 (d, J = 10.7 Hz), 128.24, 127.76, 126.87, 125.31, 124.88, 124.02, 58.42 ppm. MS m/z : 445.82.

Anal. Calcd for C₂₉H₂₀ClN₃ (%): C 78.11, H 4.52, N 9.42; found: C 78.03, H 4.74, N 9.28.

Synthesis of 10-(6-(dibenzo[b,d]furan-1-yl)pyrazin-2-yl)-9,9-diphenyl-9,10-dihydroacridine (PrFPhAc)

10-(6-chloropyrazin-2-yl)-9,9-diphenyl-9,10-dihydroacridine (2 g, 4.5 mmol), dibenzofuran-4-boronic acid (1.4 g, 6.7 mmol) and tetrakis(triphenylphosphine)-palladium(0) (Pd(PPh₃)₄, 0.35 g, 0.3 mmol) were dissolved in THF under argon, and then 2 M K₂CO₃ (THF/Water = 5/1, v/v) was added. The resulting solution was heated at 70 °C overnight. After cooled to room temperature, the mixture was evaporated to remove solvents. The residue was washed with water and extracted with dichloromethane for 3 times. The organic layer was collected and evaporated. The crude product was purified by chromatography on silica gel using petroleum ether as eluent to afford a white powder (2.3 g, 90%). ¹H NMR (400 MHz, CDCl₃): δ 9.30 (s, 1H), 8.34 (dd, *J* = 7.7, 1.2 Hz, 1H), 8.09-8.00 (m, 2H), 7.79 (dd, *J* = 8.0, 1.0 Hz, 2H), 7.75 (s, 1H), 7.69 (d, *J* = 8.2 Hz, 1H), 7.58-7.51 (m, 2H), 7.46-7.33 (m, 3H), 7.24-7.14 (m, 8H), 7.03 (dd, *J* = 7.8, 1.4 Hz, 2H), 6.99-6.92 (m, 4H) ppm. ¹³C NMR (100 MHz, CDCl₃): δ 156.07, 151.56, 146.06, 144.66, 140.84, 139.55, 138.05, 135.73, 130.44, 129.33, 127.74, 127.54, 127.08, 126.76 (d, *J* = 5.8 Hz), 125.30, 123.77, 123.36, 123.14, 122.14, 121.92, 121.22, 120.72, 111.87, 58.14 ppm. MS *m/z*: 577.62. Anal. Calcd for C₄₁H₂₇N₃O (%): C 85.25, H 4.71, N 7.27; found: C 85.52, H 4.63, N 7.38.

Synthesis of 10-(6-(dibenzo[b,d]thiophen-1-yl)pyrazin-2-yl)-9,9-diphenyl-9,10-dihydroacridine (PrTPhAc)

PrTPhAc was prepared in a similar manner with PrFPhAc. The result to afford a white powder (yield 92%). ¹H NMR (400 MHz, CDCl₃): δ 8.68 (s, 1H), 8.28 (d, *J* = 7.8 Hz, 1H), 8.24-8.20 (m, 1H), 7.96 (d, *J* = 7.5 Hz, 1H), 7.85-7.81 (m, 1H), 7.72-7.66 (m, 3H), 7.60 (t, *J* = 7.7 Hz, 1H), 7.48 (dd, *J* = 5.8, 3.0 Hz, 2H), 7.30 (t, *J* = 7.7 Hz, 3H), 7.26 (s, 2H), 7.19 (s, 1H), 7.16 (d, *J* = 8.0 Hz, 2H), 7.03 (d, *J* = 7.7 Hz, 3H), 7.00-6.94 (m, 5H) ppm. ¹³C NMR (100 MHz, CDCl₃): δ 151.14, 149.30, 144.56, 141.43, 140.96, 139.90, 138.07, 137.22, 135.94, 135.30 (d, *J* = 10.5 Hz), 134.61, 131.05, 130.53, 129.27, 127.72, 126.99 (d, *J* = 25.9 Hz), 126.69, 125.62 (d, *J* = 7.0 Hz), 124.53 (d, *J* = 8.0 Hz), 124.20, 123.80, 122.99, 122.58, 122.45 (d, *J* = 7.4 Hz), 121.43 (d, *J* = 4.4 Hz, 58.26 ppm. MS *m/z*: 593.70. Anal. Calcd for C₄₁H₂₇N₃S (%): C 82.94, H 4.58, N 7.08; found: C 83.02, H 4.33, N 7.46.

Conclusions

In conclusion, two novel donor-acceptor host materials PrFPhAc and PrTPhAc were designed and synthesized. The robust backbone and *ortho*-linkage strategy made these materials show good thermal and morphological stabilities and suitable triplet energies for red phosphorescent emitters. The difference of DBT and DBF units were also compared in several characteristics, and we found the DBF unit in this case have more positive effects to the PhOLEDs application. As a

result, high efficiencies red devices were obtained using PrFPhAc and PrTPhAc as host materials. The champion device was achieved PrFPhAc-based device with the maximum CE, PE and EQE of 36.0 cd A⁻¹, 29.1 lm W⁻¹, and 22.0%, respectively.

Acknowledgements

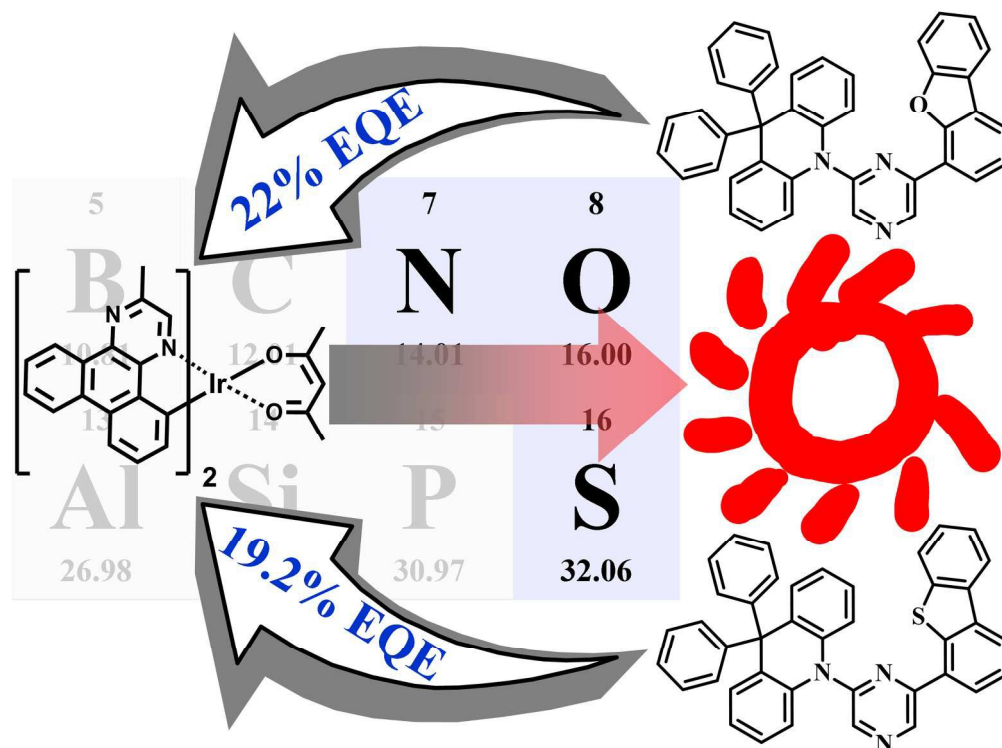
We thank to the financial support from the Natural Science Foundation of China (Nos. 61177016 and 21572152). This project is also funded by Collaborative Innovation Center (CIC) of Suzhou Nano Science and Technology, Soochow University, and by the Priority Academic Program Development of the Jiangsu Higher Education Institutions (PAPD).

Notes and references

Jiangsu Key Laboratory for Carbon-Based Functional Materials & Devices, Institute of Functional Nano & Soft Materials (FUNSOM), Soochow University
Email: zqjiang@suda.edu.cn; lsiao@suda.edu.cn*

- C. W. Tang and S. A. Van Slyke, *Appl. Phys. Lett.*, 1987, **51**, 913.
- (a) J. Kido and M. Kimura, *Science* 1995, **267**, 1332; (b) Q. Wang and D. Ma, *Chem. Soc. Rev.*, 2010, **39**, 2387; (c) M. Romain, S. Thiery, A. Shirinskaya, C. Declairieux, D. Tondelier, B. Geffroy, O. Jeannin, J. Rault-Berthelot, R. Métivier and C. Poriol, *Angew. Chem. Int. Ed.*, 2015, **54**, 1176; (d) Y. Tao, K. Yuan, T. Chen, P. Xu, H. Li, R. Chen, C. Zheng, L. Zhang and W. Huang, *Adv. Mater.*, 2014, **26**, 7931; (e) H. Wang, L. Xie, Q. Peng, L. Meng, Y. Wang, Y. Yi and P. Wang, *Adv. Mater.*, 2014, **26**, 5198; (f) L.-S. Cui, Y. Liu, X.-D. Yuan, Q. Li, Z.-Q. Jiang and L.-S. Liao, *J. Mater. Chem. C*, 2013, **1**, 8177; (g) L. Ding, S.-C. Dong, Z.-Q. Jiang, H. Chen, L.-S. Liao, *Adv. Funct. Mater.*, 2015, **25**, 645; (h) X.-Y. Liu, F. Liang, L. Ding, S.-C. Dong, Q. Li, L.-S. Cui, Z.-Q. Jiang, H. Chen and L.-S. Liao, *J. Mater. Chem. C*, 2015, **3**, 9053; (i) X.-Y. Liu, F. Liang, L.-S. Cui, X.-D. Yuan, Z.-Q. Jiang and L.-S. Liao, *Chem. Asian J.*, 2015, **10**, 1402; (j) X.-Y. Liu, F. Liang, L. Ding, Q. Li, Z.-Q. Jiang and L.-S. Liao, *Dyes Pigments*, 2016, **126**, 131.
- M. Pope and C. E. Swenberg, *Electronic Processes in Organic Crystals and Polymers*, Oxford University Press, New York, 1999.
- (a) Y. Ma, H. Zhang, J. Shen and C. Che, *Synth. Met.*, 1998, **94**, 245; (b) M. A. Baldo, D. F. O'Brien, Y. You, A. Shoustikov, S. Sibley, M. E. Thompson and S. R. Forrest, *Nature* 1998, **395**, 151; (c) M. A. Baldo, S. Lamansky, P. E. Burrows, M. E. Thompson and S. R. Forrest, *Appl. Phys. Lett.*, 1999, **75**, 4; (d) S. Reineke, K. Walzer and K. Leo, *Phys. Rev. B*, 2007, **75**, 125328; (e) M. Kim and J. Y. Lee, *Adv. Funct. Mater.*, 2014, **24**, 4164.
- (a) L.-X. Xiao, Z.-J. Chen, B. Qu, J.-X. Luo, S. Kong, Q.-H. Gong and J. Kido, *Adv. Mater.*, 2011, **23**, 926; (b) Y.-T. Tao, C.-L. Yang and J.-G. Qin, *Chem. Soc. Rev.*, 2011, **40**, 2943; (c) K.-S. Yook and J.-Y. Lee, *Adv. Mater.*, 2012, **24**, 3169; (d) H. Xu, R. Chen, Q. Sun, W. Lai, Q. Su, W. Huang and X. Liu, *Chem. Soc. Rev.*, 2014, **43**, 3259; (e) W. Wong and C. Ho, *Coord. Chem. Rev.*, 2009, **253**, 1709.
- (a) D. H. Kim, N. S. Cho, H.-Y. Oh, J. H. Yang, W. S. Jeon, J. S. Park, M. C. Suh and J. H. Kwon, *Adv. Mater.*, 2011, **23**, 2721; (b) C.-

- L. Ho, H. Li and W.-Y. Wong, *J. Organomet. Chem.*, 2014, **751**, 261;
(c) C. Han, L. Zhu, J. Li, F. Zhao, Z. Zhang, H. Xu, Z. Deng, D. Ma and P. Yan, *Adv. Mater.*, 2014, **26**, 7070.
- 7 D. Song, S. Zhao, Y. Luo and H. Aziz, *Appl. Phys. Lett.*, 2010, **97**, 243304.
- 8 (a) R. Wang, D. Liu, R. Zhang, L. Denga and J. Li, *J. Mater. Chem.*, 2012, **22**, 1411; (b) Z. Zhang, Z. Zhang, R. Chen, J. Jia, C. Han, C. Zheng, H. Xu, D. Yu, Y. Zhao, P. Yan, S. Liu and W. Huang, *Chem. Eur. J.*, 2013, **19**, 9549; (c) K. Wang, F. Zhao, C. Wang, S. Chen, D. Chen, H. Zhang, Y. Liu, D. Ma and Y. Wang, *Adv. Funct. Mater.*, 2013, **23**, 2672; (d) H. Wang, L. Meng, X. Shen, X. Wei, X. Zheng, X. Lv, Y. Yi, Y. Wang and P. Wang, *Adv. Mater.*, 2015, **27**, 4041; (e) J. Ye, C.-J. Zheng, X.-M. Ou, X.-H. Zhang, M.-K. Fung and C.-S. Lee, *Adv. Mater.*, 2012, **24**, 3410; (f) S. J. Su, C. Cai and J. Kido, *Chem. Mater.*, 2011, **23**, 274; (g) C. S. Oh, C. W. Lee and J. Y. Lee, *Chem. Commun.*, 2013, **49**, 3875; (h) D.-S. Leem, S. O. Jung, S.-O. Kim, J.-W. Park, J. W. Kim, Y. -S. Park, Y.-H. Kim, S.-K. Kwon and J.-J. Kim, *J. Mater. Chem.*, 2009, **19**, 8824; (i) C.-H. Chen, L.-C. Hsu, P. Rajamalli, Y.-W. Chang, F.-I. Wu, C.-Y. Liao, M.-J. Chiu, P.-Y. Chou, M.-J. Huang, L.-K. Chu and C.-H. Cheng, *J. Mater. Chem.*, 2014, **2**, 6183.
- 9 (a) K. Brunner, A. van Dijken, H. Börner, J. J. A. M. Bastiaansen, N. M. M. Kiggen and B. M. W. Langeveld, *J. Am. Chem. Soc.*, 2004, **126**, 6035; (b) S.-J. Su, C. Cai and J. Kido, *J. Mater. Chem.*, 2012, **22**, 3447.
- 10 (a) H. Uoyama, K. Goushi, K. Shizu, H. Nomura and C. Adachi, *Nature* 2012, **492**, 234; (b) Q. Zhang, J. Li, K. Shizu, S. Huang, S. Hirata, H. Miyazaki and C. Adachi, *J. Am. Chem. Soc.*, 2012, **134**, 14706; (c) Q. Zhang, B. Li, S. Huang, H. Nomura, H. Tanaka and C. Adachi, *Nat. Photonics* 2014, **8**, 326; (d) Q. Zhang, H. Kuwabara, W. J. Potscavage, S. Huang, Y. Hatae, T. Shibata and C. Adachi, *J. Am. Chem. Soc.*, 2014, **136**, 18070; (e) Y. J. Cho, K. S. Yook and J. Y. Lee, *Adv. Mater.*, 2014, **26**, 6642.
- 11 Y.-K. Wang, Y.-L. Deng, X.-Y. Liu, X.-D. Yuan, Z.-Q. Jiang and L.-S. Liao, *Dyes Pigments*, 2015, **122**, 6.
- 12 (a) A. D. Becke, *J. Chem. Phys.*, 1993, **98**, 5648; (b) C. Lee, W. Yang and R. G. Parr, *Phys. Rev. B*, 1988, **37**, 785.



190x142mm (300 x 300 DPI)